Electronic Supplementary Material (ESI) for Journal of Materials Chemistry A.

Anti-corrosive hierarchical structured copper mesh film with superhydrophilicity and underwater low adhesive superoleophobicity for highly efficient oil/water separation

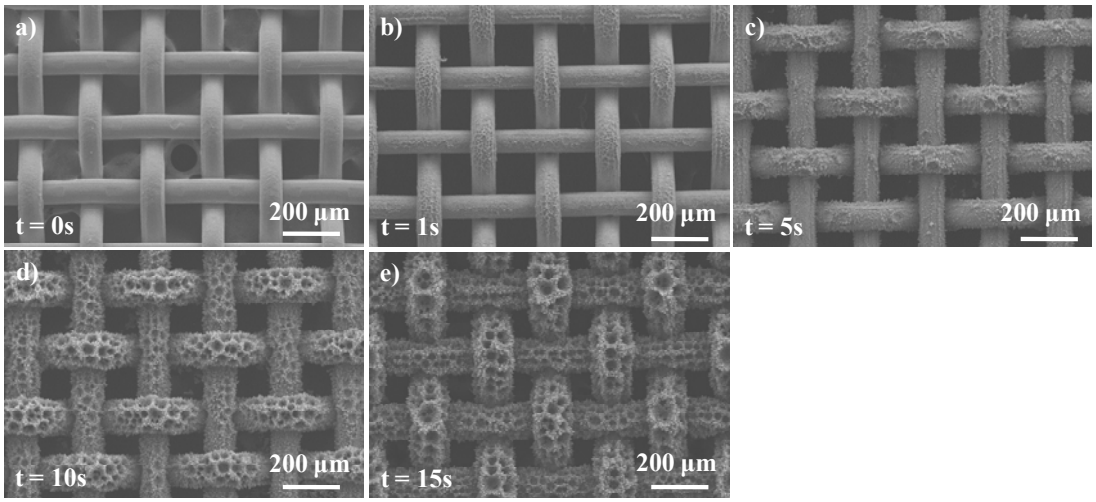

Figure S1. SEM images of copper mesh substrates after electrodeposition for different times. From these pictures it can be seen that with increasing the electrodeposition time, more and more nanostructures can be produced on the substrates, after about 15s, the substrates would be covered by the hierarchical structures completely. Therefore, in this work, the electrodeposition time for preparation of hierarchical structures was fixed at 15s.

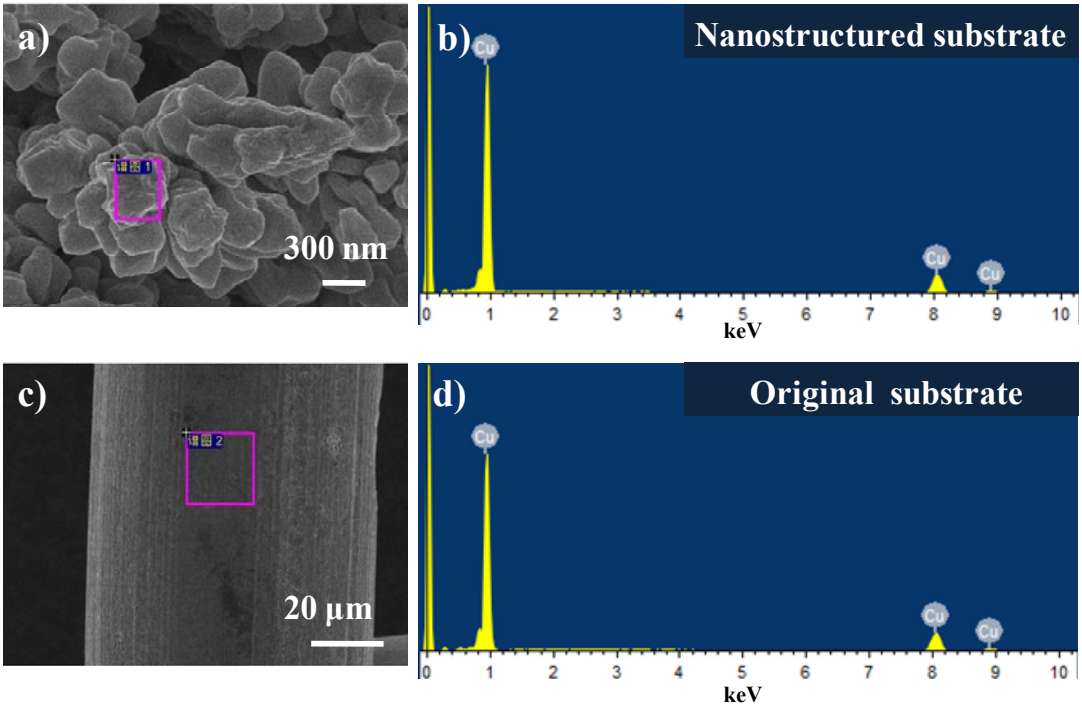

Figure S2. (a) and (c) are the SEM images of the nanostructured copper mesh film and the original copper mesh substrate, respectively. (b) and (d) are the EDS results corresponding to (a) and (c), respectively. These results indicate that after electrodeoposition, the chemical composition on the film has no variation, and the hierarchical structures are composed of elementary Cu, which is consistent with the XRD results in Figure 1f.

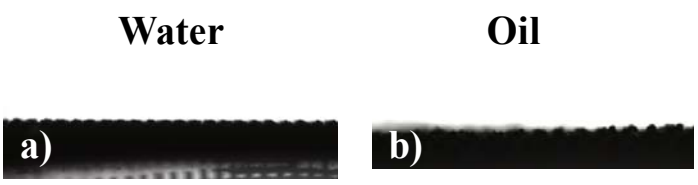

Figure S3. Shapes of a water droplet (a) and oil droplet (b, 1, 2-dichloroethane) on the as-prepared film, indicating that the film is superhydrophilic and superoleophilic in air.

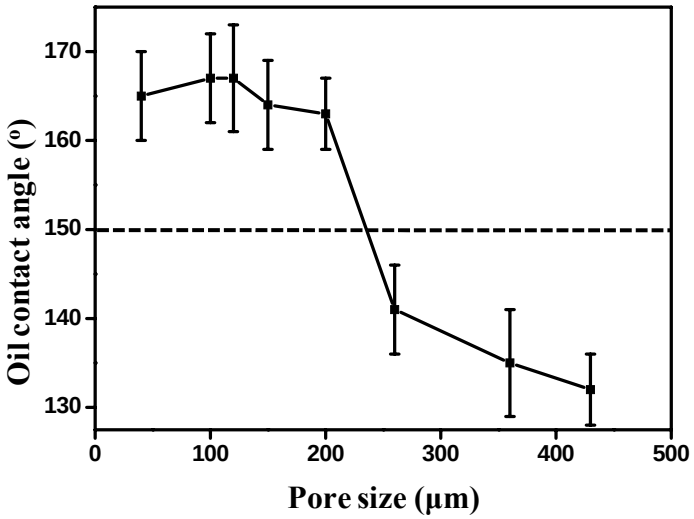

Figure S4. Dependence of underwater oil contact angle on the pore size of the copper mesh substrates. It can be concluded that substrates with pore size smaller than 200 μm are proper for realization of underwater superoleophobicity.

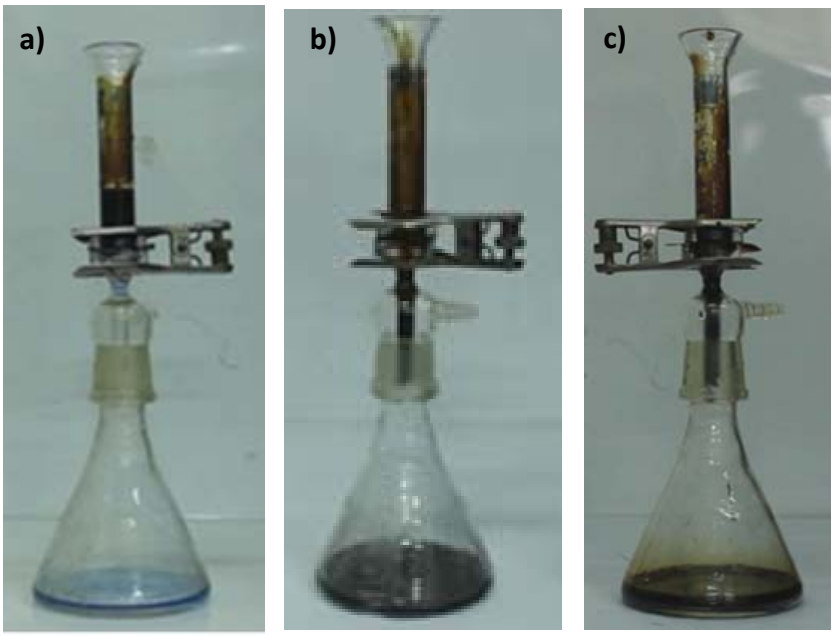

Figure S5. Photographs of oil/water separation on water wetted (a), oil wetted (b), and dry film (c), respectively. It can be seen that the mixture can only be separated on water wetted film, more details see movie 1 and movie 2 and movie 3.

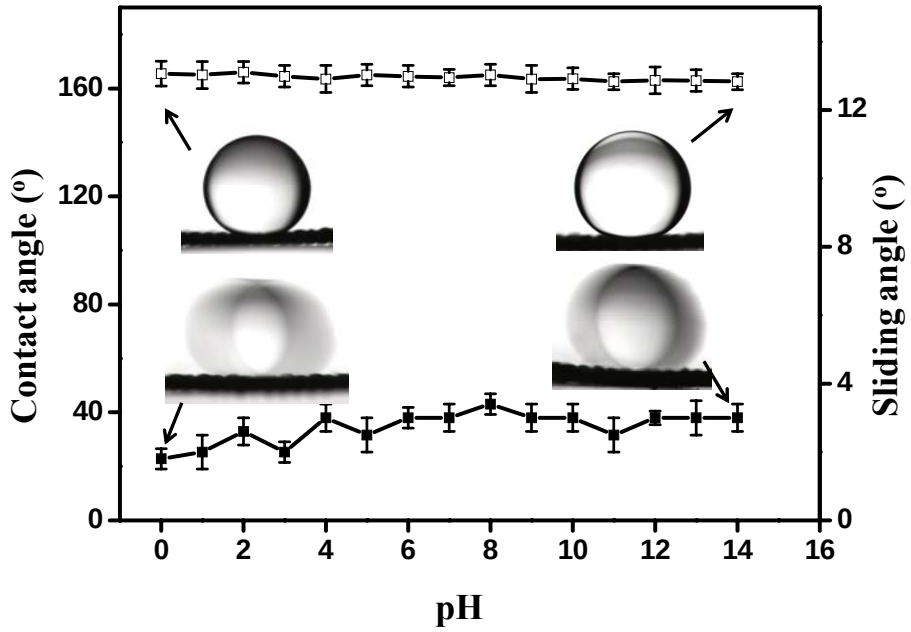

Figure S6. Oil contact angles and sliding angles on the nanostructured film after immersion in water solutions with pH from 0 to 14. Insets are the photographs on an oil droplet on the film in corresponding solutions. It can be seen that the underwater superoleophobic and low adhesive properties can be observed for water solution with all pH range, demonstrating a good acid/basic-resisting ability of the film.

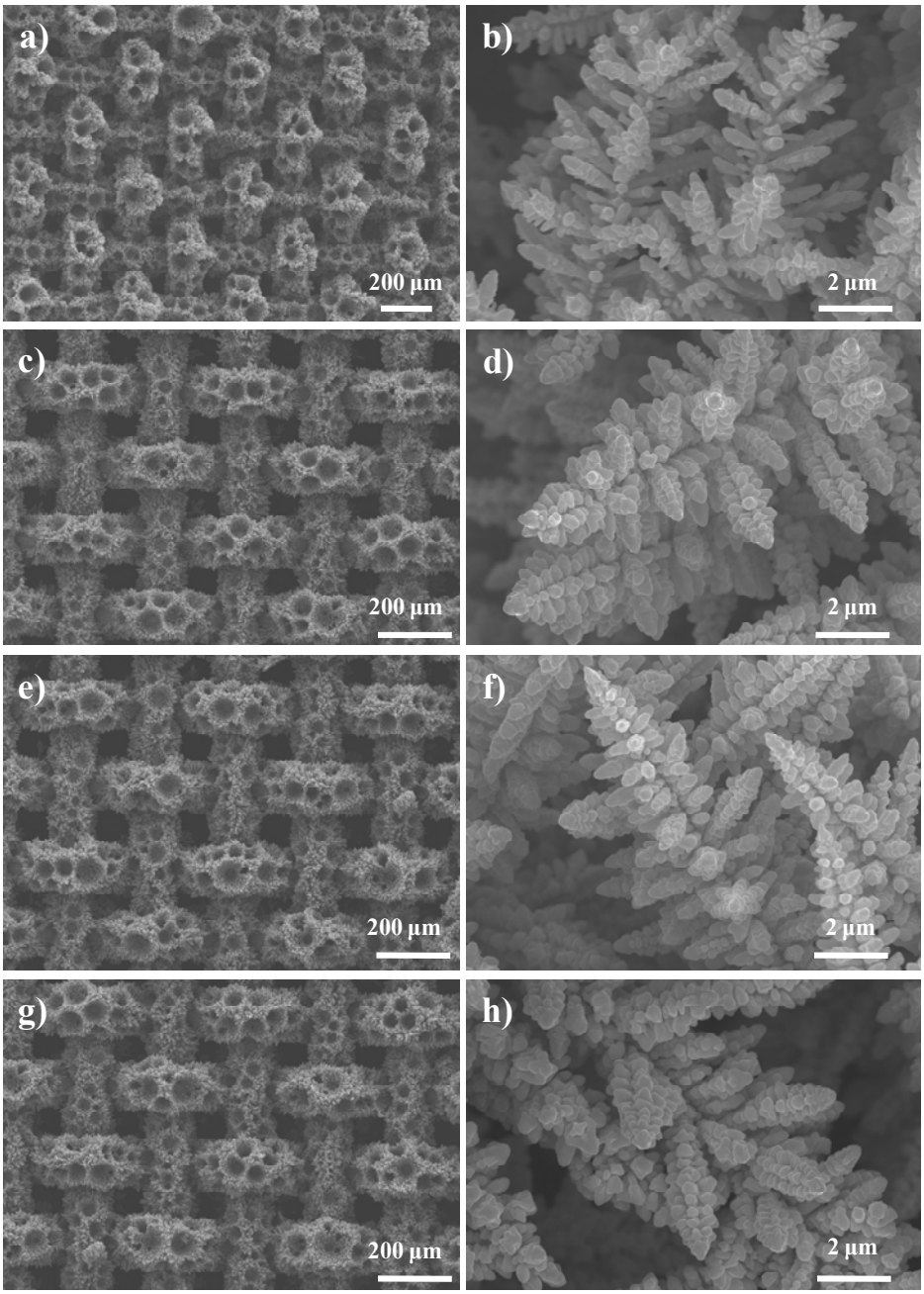

Figure S7. SEM images of nanostructured copper mesh substrates after immersion in HCl solution with different concentrations and different hours: (a) 1M, 24h; (c) 1M, 48h; (e) 2M 24h; (g) 2M 48h. (b), (d), (f) and (h) are the amplified images corresponding to (a), (c), (e) and (g), respectively. Compared with original nanostructured surface (Figure 1), it can be seen that after immersion, there is no apparent variation of the microstructures can be seen.

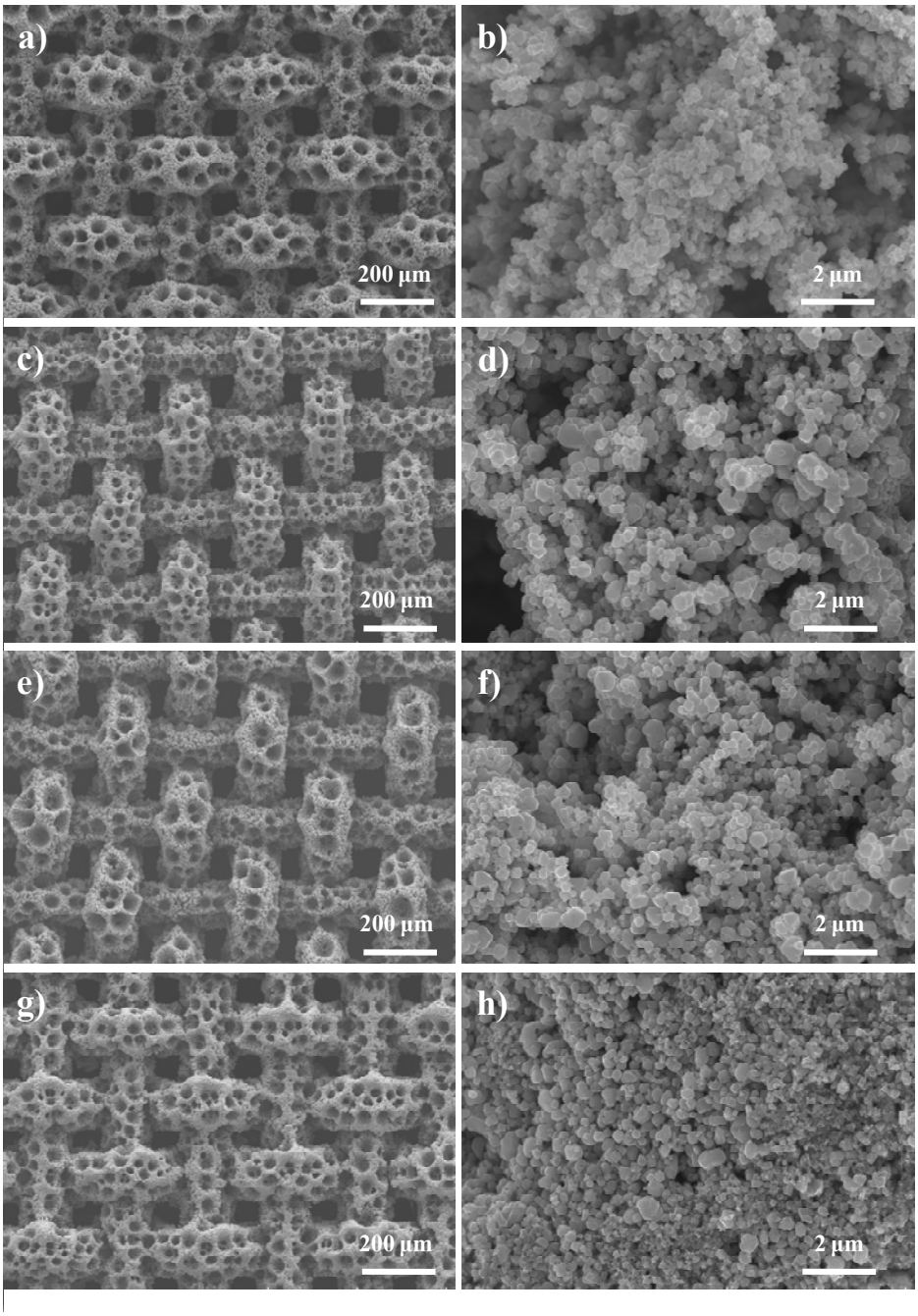

Figure S8. SEM images of nanostructured copper mesh substrates after immersion in NaOH solution with different concentrations and different hours: (a) 1M, 24h; (c) 1M, 48h; (e) 2M 24h; (g) 2M 48h. (b), (d), (f) and (h) are the amplified images corresponding to (a), (c), (e) and (g), respectively. From these images, one can observe that after immersion in NaOH solution, although the original dendritical structures disappear, and unordered nanoparticles aggregate together (magnified

images in Figure S7), the hierarchical porous structures can still be remained (Figure S7a, c, e, g).

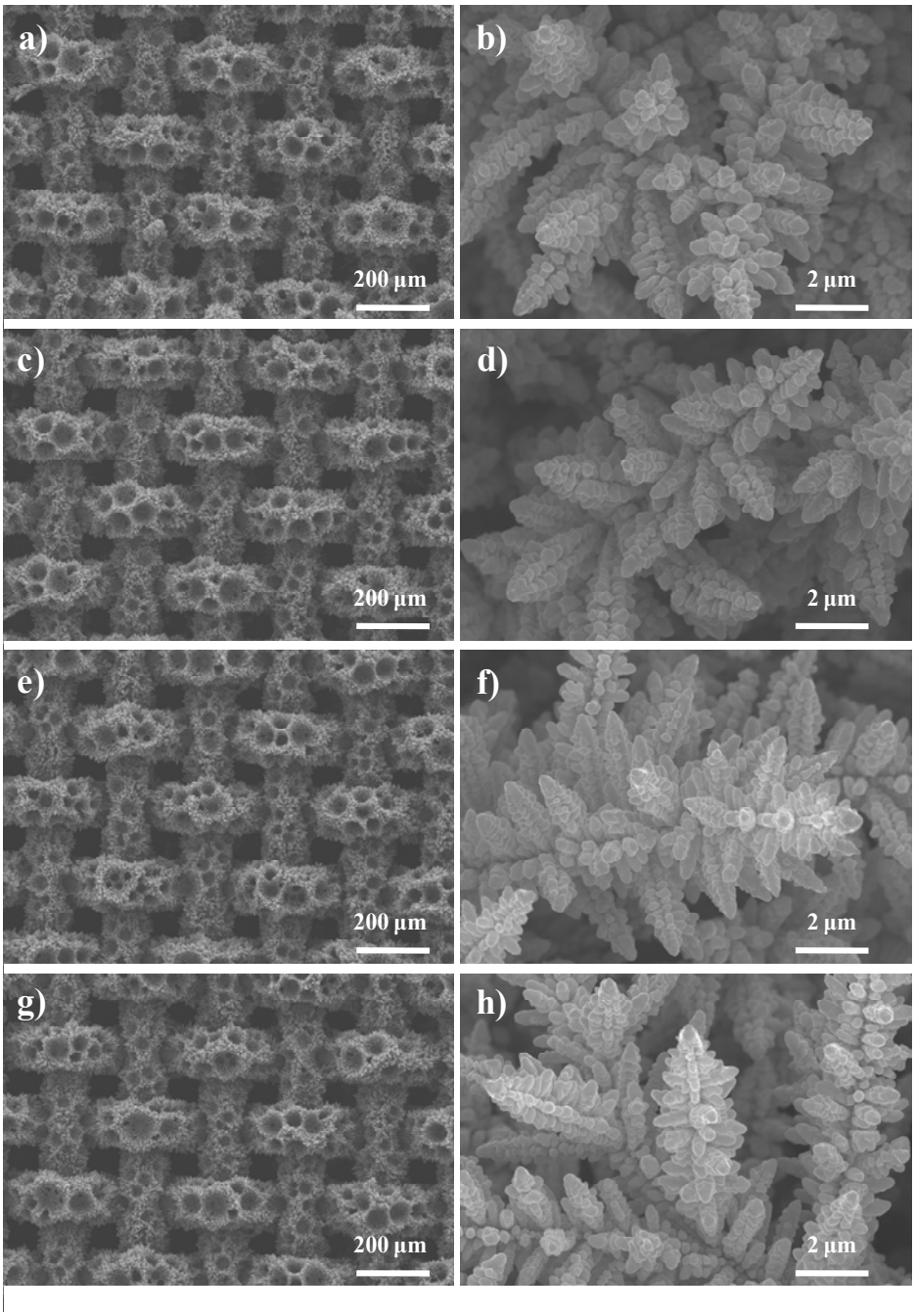

Figure S9. SEM images of nanostructured copper mesh substrates after immersion in NaCl solution with different concentrations and different hours: (a) 10 wt%, 24h; (c) 10 wt%, 48h; (e) 20 wt%, 24h; (g) 20 wt%, 48h. (b), (d), (f) and (h) are the amplified images corresponding to (a), (c), (e) and (g), respectively. It can be seen that after

immersion in NaCl solution, there is no apparent variation of the surface microstructures compared with original nanostructured surface.

Table S1. Oil/water interfacial tension in different corrosive solutions (1, 2-dichloroethane was used as the test oil).

	1M HCl	1MNaOH	wt 10% NaCl
γ(dyn cm^{-1})	29.6	14.2	20.9

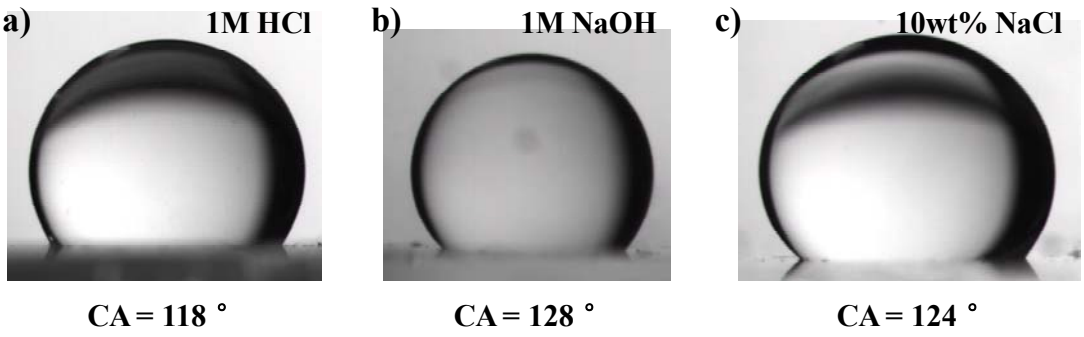

Figure S10. Photograph of an oil droplet (1, 2-dichloroethane) on flat copper surfaces in different corrosive solutions.

Discussion about the variation of oil contact angles and separation efficiency (results in Figure 7) after immersion in corrosive solutions

According to Jiang's report,[1] for polar oil droplet (in Figure 7a, the oil is polar1, 2-dichloroethane), the underwater oil contact angle is mainly controlled by the oil/water interfacial tension. Herein, the oil/water interfacial tension was measured and as shown in Table S1, for different water solutions, the oil/water interfacial tension is different, which would result in different wetting performances for oil

droplet on the flat copper surface (Figure S10). From the above, it can be concluded that in different corrosive solutions, the underwater oil contact angles on flat copper surfaces are different due to the different oil/water interfacial tensions. However, on the hierarchical structured copper mesh film, such limited wetting differences (the difference of contact angles on flat surface is no more than 10°) would be undistinguishable after amplification by the hierarchical structures. Therefore, as shown in Figure 7a, the oil contact angles for these solutions are similar with each other.

After immersion into different corrosive solutions, although all the films displays high oil/water separation efficiency (higher than 99%, Figure 7b), there are some tiny differences between different solutions, and the differences may be due the different microstructures on these films. For film after immersion in HCl and NaCl solutions, the microstructures have no apparent variation, thus, the separation efficiency has no apparent change compared with original film (Figure 5). On the film after immersion in NaOH solution, some corrosive phenomenon can be observed, although hierarchical structures are still present, the nanoscale structures have been destroyed, and this may be responsible for the relative low separation efficiency.

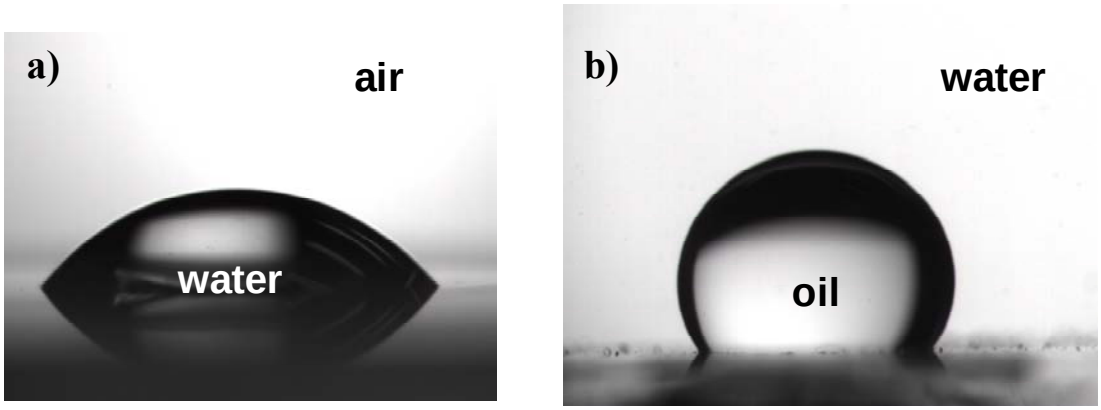

Figure S11. (a) Photograph of a water droplet on the flat copper film with a contact angle of about 53°; (b) Photograph of an oil droplet (1, 2-dichloroethane) on the flat copper mesh film in water with a contact angle of about 120°.

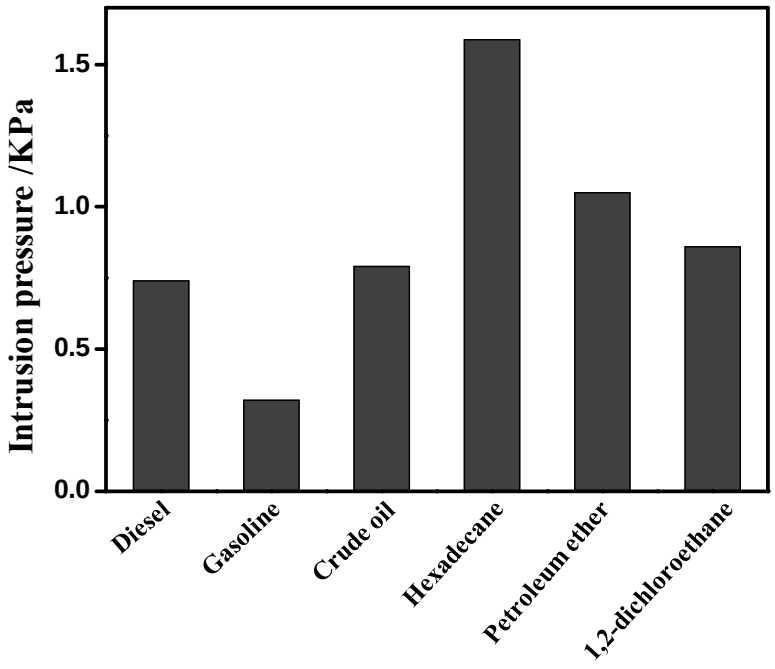

Figure S12. Theoretical intrusion pressure of different oils on the film.

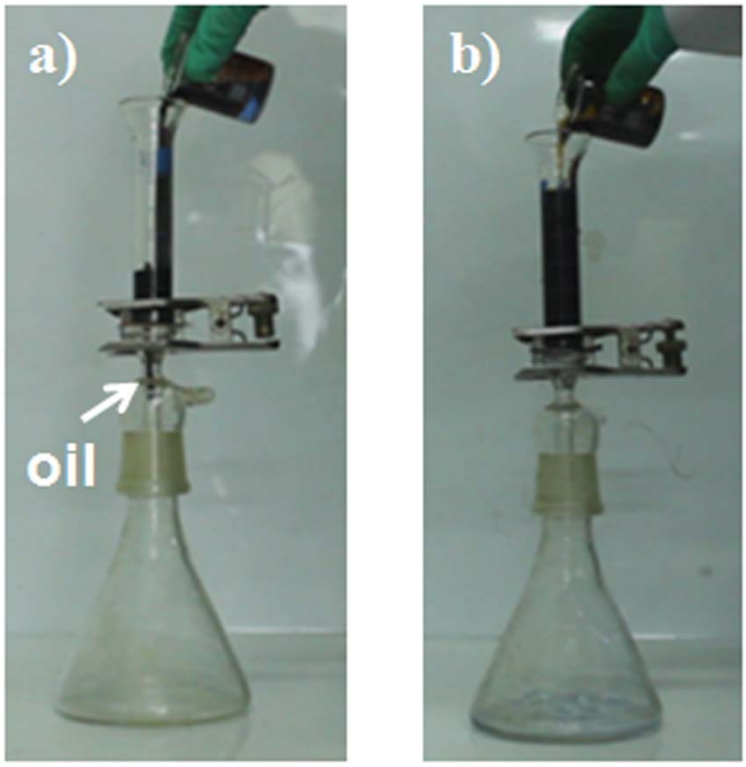

Figure S13. Photographs of oil/water separation on the water wetted copper mesh film without (a) and with (b) hierarchical structures.

In this work, oil/water separation was also investigated on the water wetted copper mesh film without nanostructures, as shown in Figure S13a, when the liquid height is added to some extent, the oil would permeate the film and flow into the conical flask. As a comparison, on the film with nanostructures, it can be seen that even when more mixture was added, the oil was still kept above the film, indicating that the film with nanostructures can stand higher oil pressure compared with the film without nanostructures. The results can also help to explain why the experimental intrusion pressure (Figure 6) is higher than the theoretical values (Figure S12). Because the theoretical values are calculated based on the hypothesis that the only micrometer scale pores are present, which is similar with the copper mesh film without nanostructures in Figure S13a. From the above, we can conclude that the introduction

of nanostructures onto the copper mesh substrates can help to increase the bearing force and the stability of the separating device. (More details please see movie 1 and movie 3).

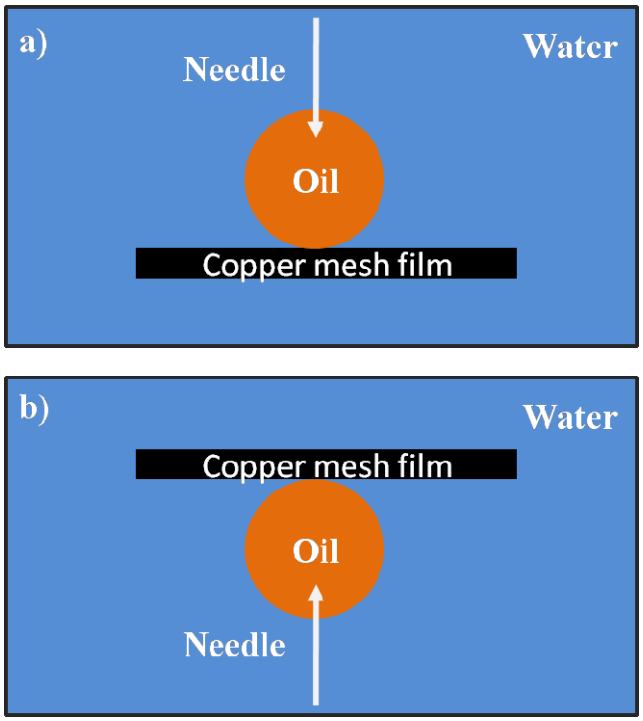

Scheme 1. Illustration of examination of underwater oil contact angle: a) for oils with higher density than water; (b) for oils with lower density than water, respectively. The methods used here for investigation of underwater oil contact angle also have been used in other reports. For oils with higher density than water, please see refence 2-3, for oils with lower density than water, please see reference 4-5.

Reference

1 M. Liu, Z. Xue, H. Liu, L. Jiang, *Angew. Chem. Int. Ed*. 2012, **51**, 8348.

2 M. Liu, S. Wang, Z. Wei, Y. Song, L. Jiang, 2009, **21**, 665.

3 M. Jin, S. Li, J. Wang, Z. Xue, M. Liao, S. Wang, Chem. Commun., 2012, **48**, 11745.

4 V. Hejazi, A. E. Nyong, P. K. Rohatgi, M. Nosonovsky, *Adv. Mater.* 2012, **24**, 5963.

5 Y. C. Jung, B. Bhushan, Langmuir, 2009, **25**, 14165.